Applications of Synthetic Aperture Radar to Meteorology and Oceanography Command Operations

Todd D. Sikora
Millersville University
P.O. Box 1002
Millersville, PA 17551-0302
phone: (717) 872-3292 fax: (717) 871-4725 email: Todd.Sikora@millersville.edu

Grant Number: N00014-06-1-0046

LONG-TERM GOALS

This annual report covers research also conducted by George S. Young and Nathanial S. Winstead under now-expired ONR grants (N00014-07-1-0934 and N00014-07-1-0577, respectively). Our long-term goal was to employ near-surface wind speed, derived from synthetic aperture radar (SAR) images of the sea surface, as a marine meteorological research and forecasting tool. That is, we aimed to use SAR-derived wind speed (SDWS) images to discover dynamical and morphological characteristics of microscale, mesoscale, and synoptic scale marine meteorological phenomena. We also aimed to demonstrate how the fruits of our discovery can aid marine meteorological analysts and forecasters.

OBJECTIVES

Our objectives were to:

1. Develop software tools for portable, automated analysis of SDWS images with the objective of resolving intense mesoscale variability within those images.

2. Develop an SDWS-based system for automated verification of, and error warning for, mesoscale near-surface wind field forecasts produced by numerical weather prediction (NWP) models. The emphasis is on verification and error detection in those regions most challenging to mesoscale NWP models—namely, the near-shore zones adjacent to complex topography.

3. Empirically and theoretically investigate the SDWS-signature of convectively-driven squall / lull couplets. The analysis includes the forcing, structure, and predictability of these intense mesoscale variations in the near-surface wind speed field. The goal is to make incremental gains towards improved NWP model and statistical forecasts of this phenomenon.

In the context of these objectives, we outlined five tasks:

1. Develop a highly portable, efficient, and verifiable CMOD 4/5 hybrid software system for SDWS retrieval.

2. Develop a fully automated system for mapping intense mesoscale variability in SDWS images.

3. Determine the forcing, structure, and predictability of the convectively-driven open ocean squall / lull couplet features frequently seen within SDWS images.

4. Develop an SDWS-based system for automated verification of, and error warning for, mesoscale near-surface wind field forecasts produced by NWP models.

5. Publish results in appropriate journals and present research at relevant conferences.

APPROACH

The basis for our research was the plethora of SDWS image frames from the Bering Sea, Gulf of Alaska, East Coast of the United States, and the North Atlantic Ocean (from 1998 to present) contained in an archive at The Johns Hopkins University Applied Physics Laboratory (JHUAPL). This data was provided at no cost by Dr. Winstead of JHUAPL. The image archive has been used extensively by the PIs to study atmospheric phenomena in the Gulf of Alaska.

Recall the project is organized as a series of tasks. The work corresponding to Tasks 1 through 4 was completed in previous years and those results are described in detail in previous annual reports. Task 5 is ongoing as of the time of this writing, with one remaining manuscript in review (*Winstead et al.*, submitted).

WORK COMPLETED

Task 1: Completed in a previous year.

Task 2: Completed in a previous year.

Task 3: Completed in a previous year.

Task 4: Completed in a previous year.

Task 5: Two journal articles were published (see Publications, Section b., for details) and a third is under review. In addition, we presented our results from Task 4 at the American Meteorological Society's Seventeenth Conference on Air-Sea Interaction (*Young et al.* 2012).

RESULTS

Task 1: Covered in a previous annual report.

Task 2: Covered in a previous annual report.

Task 3: Covered in a previous annual report.

Task 4: Covered in a previous annual report.

IMPACT/APPLICATIONS

Research completed in Tasks 1 through 4 fulfills ONR objectives by making progress towards the automated integration of standard meteorological NWP model output and SAR data. The combination of Tasks 1 and 2 provides high-resolution analyses of near-surface wind speed, direction, and gust intensity in *in situ* data-sparse regions over the ocean, including the littoral zone. Task 4 leverages that information to use SDWS to assess the location, scale, and magnitude of near-surface wind field errors in NWP models. The observational results associated with Task 3 will lead to improved forecasts of both near-surface wind and other meteorological and oceanographic variables which can be deduced from the spatial pattern of mesoscale wind speed variability.

RELATED PROJECTS

In the course of our research on SAR detection of mesoscale severe wind events over high latitude seas we've come across a number of intense synoptic scale cyclones, often with bands of strong winds either spiraling into or circling the storm center. These wind bands typically have a strong gradient on the side towards the storm center, corresponding to occluded and secluded fronts on National Weather Service analyses (*Young et al.* 2005). To examine the three-dimensional structure associated with these striking patterns gale-force winds, we simulated one of these "Aleutian Low" cases (Figure 1) using the Weather Research and Forecasting (WRF) model. Dr. Winstead configured WRF and ran the simulations while Dr. Young undertook the three-dimensional visualization and analysis. WRF was run with four nested grids (54, 18, 6, and 2 km), the finest providing resolution approaching that of SDWS.

The WRF surface wind field (Figure 2) reveals an occluded front wrapping into the cyclone center with a band of strong winds (the cold conveyor belt) located on the outer side of the occluded front, just as depicted in the SDWS image. Three dimensional analyses of the wind, temperature, humidity, stability, and potential vorticity fields reveal that the cyclone is vertically stacked throughout the troposphere and lower stratosphere, as would be expected for a mature system. A surprising finding is that the cyclone is warm core throughout its depth. This structure has not been observed in the mid-latitude cyclones that we examined in prior studies. It may reflect the low tropopause level typical of high latitudes as well as this cyclone's strong perturbation of the tropopause height. Because of this thermal structure, the cyclone's inner wind field is strongest at the surface and in the lower troposphere rather than near the tropopause as observed in conventional cold core mature cyclones. Only well to the east of the cyclone center, along the warm and cold fronts, does the thermal wind follow the conventional baroclinic pattern leading to a jet stream at tropopause level.

Another surprising finding from this case is the extent to which tropopsheric air from the cyclone's warm sector is injected into the stratosphere over the occluded front. Indeed, cross sections of moisture (not shown) reveal that the moisture tropopause north of the cyclone is deformed upward as strongly as the moisture tropopause near the cyclone center is deformed downward. The result is a nearly vertical, and in some places inverted, moisture tropopause circling the cyclone center. Buoyantly driven spreading of this branch of the warm conveyor belt over the occluded front vertically compresses the isentropic layers resulting in the stability-based tropopause being far less distorted than the moisture-based tropopause. Basically, the warm, moist air of the warm conveyor belt rises to its level of neutral buoyancy at stratospheric levels and then spreads laterally (mostly away from the cyclone center) to achieve stabilities commensurate with the stratosphere while still maintaining moisture far in excess of the stratospheric norm. Thus, the arm of the warm conveyor belt spiraling into this cyclone along the occluded front leads to a massive transport of tropospheric air from the cyclone's warm sector into the stratosphere around the cyclone core. The implications for troposphere/stratosphere chemical exchange are far reaching.

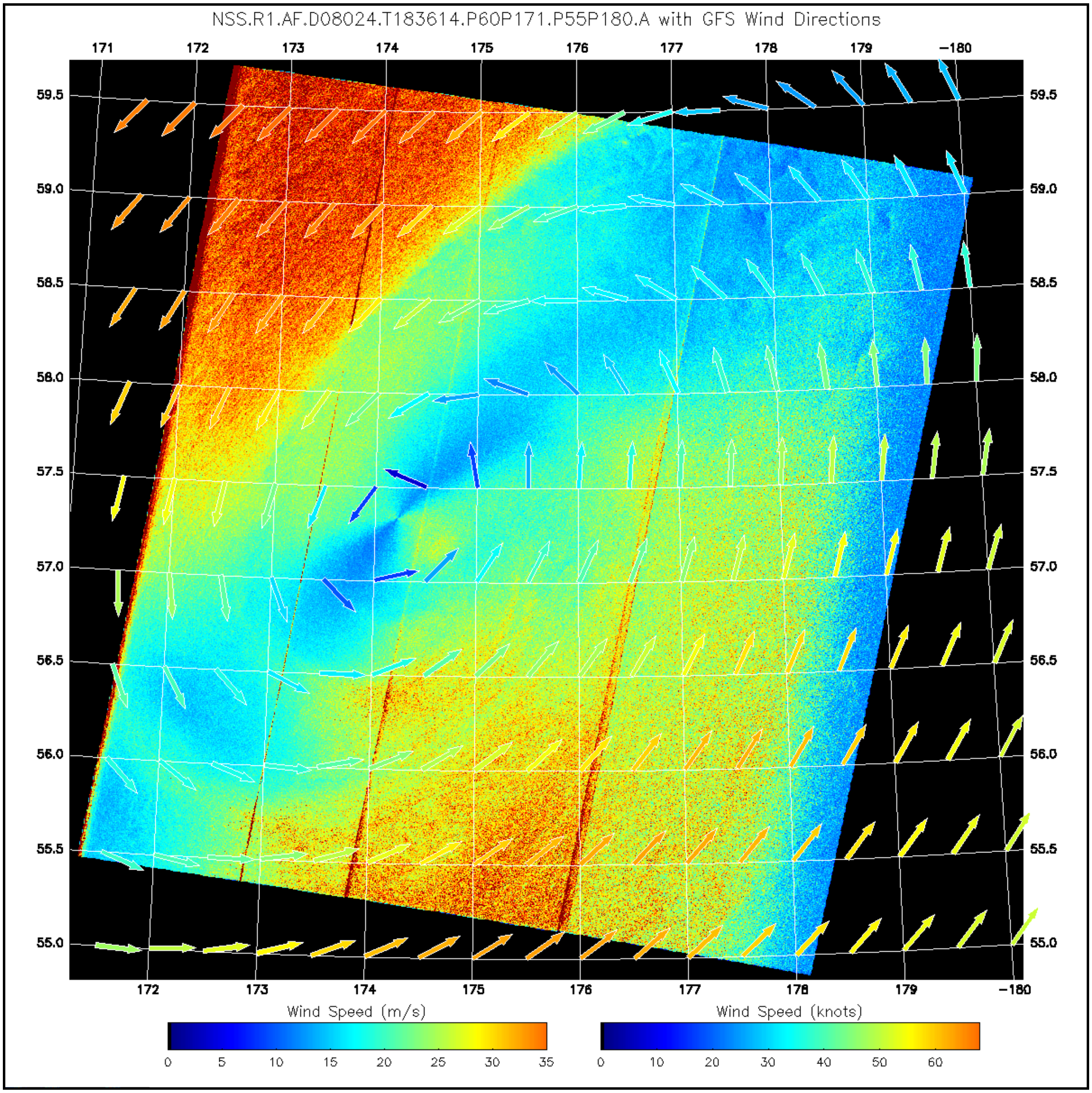

Figure 1. SDWS overlaid by GFS-analyzed surface wind vectors depict a conveyor belt of large wind speed spiraling into the center of a mature cyclone in the Bering Sea at 1836 UTC on 24 January 2008. (Provided courtesy of JHUAPL)

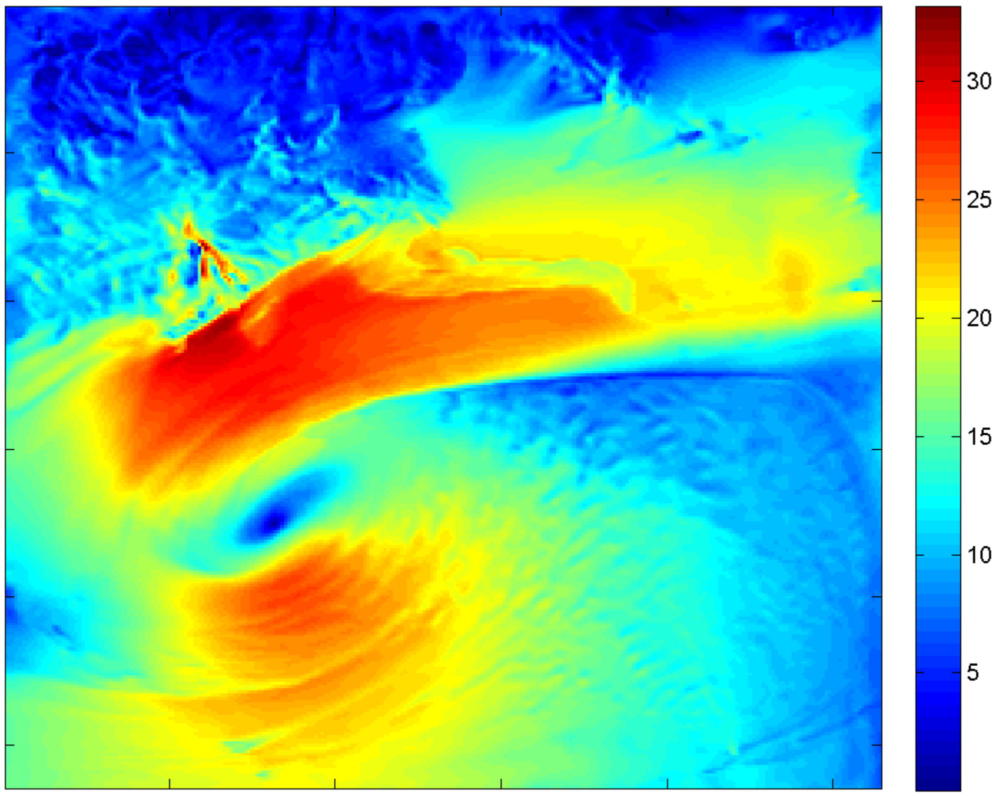

Figure 2. WRF surface wind speed (ms^{-1}) corresponding to the cyclone imaged in Figure 1 at 1700 UTC on 24 January 2008.

Dr. Sikora continued his collaboration with Canadian scientists in the development of the Spaceborne Ocean Intelligence Network. That research aims to automate the SAR detection of sea surface temperature (SST) fronts. Automated classification of the signatures of atmospheric and oceanic processes in SAR images of the ocean surface has been a difficult problem, due in part to the fact that different processes can produce signatures that are very similar in appearance. For example, brightness fronts that are the signatures of horizontal wind shear (WIN) caused by atmospheric processes that occur independently of properties of the ocean often appear very similar to brightness fronts that are signatures of SST fronts. Using MODIS-derived SST for validation, 302 SAR SST and 193 SAR WIN signatures were collected from over 250 RADARSAT-2 images of the Gulf Stream region using a Canny edge detector. A vector consisting of textural and contextual features was extracted from each signature and used to train and test logistic regression, maximum likelihood, and binary tree classifiers. Following methods proven effective in the analysis of SAR images of sea-ice, textural features included those computed from the gray-level co-occurrence matrix for regions along and astride each signature. Contextual features consisted of summaries of the wind vector field near each signature. Results indicate that signatures labeled SST can be automatically discriminated from signatures labeled WIN using the mean wind direction with respect to a brightness front with an accuracy of between 80 and 90 percent. The results have been submitted for publication in the *Journal of Atmospheric and Oceanic Technology* (*Jones et al.* submitted).

REFERENCES

Jones, C.T., T.D. Sikora, P.W. Vachon, J. Wolfe, and B. DeTracey: Automated classification of brightness fronts in RADARSAT-2 images of the ocean. Submitted to *J. Atmos. Oceanic Technol.*, **29**, 89-102.

Winstead, N.S., G.S. Young, and T.D. Sikora: Demonstration of the use of synthetic aperture radar-determined wind speed in numerical weather prediction error detection. Submitted to *National Weather Digest*.

Young, G.S., T.D. Sikora, and N.S. Winstead, 2005: Use of synthetic aperture radar in fine-scale surface analysis of synoptic-scale fronts at sea. *Wea. Forecasting*, **20**, 311-327.

Young, G.S., N.S. Winstead and T.D. Sikora, 2012: The use of synthetic aperture radar-derived wind speed in numerical weather prediction error detection. *Seventeenth Conference on Air-Sea Interaction*, American Meteorological Society (AMS), Boston, MA, 9-13 July 2012.

PUBLICATIONS

a. Previously reported:

Fisher, C.M., G.S. Young, N.S. Winstead, and J.D. Haqq-Misra, 2008: Comparison of synthetic aperture radar-derived wind speeds with buoy wind speeds along the mountainous Alaskan coast. *J. Appl. Meteor. Climatol.,* **47** 1365 - 1376. [published, refereed]

Fisher, C.M., 2007: Remote Sensing of High Latitude Open Cell Convection. Penn State M.S. thesis. [published]

Sikora, T.D., G.S. Young, M.D. Stepp, and C.M. Fisher, 2011: A synthetic aperture radar-based climatology of open cell convection over the Northeast Pacific Ocean. *J. Appl. Meteor. Climatol.*, **50**, 594-603. [published, refereed]

Sikora, T.D., G.S. Young, and N.S. Winstead, 2006: Manual and semi-automated wind direction editing for use in the generation of synthetic aperture radar wind speed imagery. *Proceedings, OceanSAR 2006*, St. John's, Newfoundland, Canada, 23-25 October 2006. [published]

Swales, D.J., 2009: Shear driven gravity waves on a sloping front. Penn State M.S. thesis. [published]

Young, G.S., T.D. Sikora, and C.M. Fisher, 2007: Use of MODIS and synthetic aperture radar wind speed imagery to describe the morphology of open cell convection. *Can. J. Remote Sens.*, **33**, 357-367. [published, refereed]

Young, G.S., T.D. Sikora, and N.S. Winstead, 2007: Manual and semi-automated wind direction editing for use in the generation of synthetic aperture radar wind speed imagery. *J. Appl. Meteor. Climatol.*, **46**, 776-790. [published, refereed]

Young, G.S., T.D. Sikora, and N.S. Winstead, 2008: Mesoscale near-surface wind speed variability mapping with synthetic aperture radar. *Sensors,* **8**, 7012-7034. [published, refereed]

Young, G.S., N.S. Winstead, and T.D. Sikora, 2010: A SAR-based error warning product. *Preprints, Seventeenth Conference on Satellite Meteorology and Oceanography*, AMS, Annapolis, MD, 27-30 September 2010. [published]

b. New or status changed:

Jones, C.T., T.D. Sikora, P.W. Vachon, and J. Wolfe, 2012: Towards automated identification of sea surface temperature front signatures in Radarsat-2 images. *J. Atmos. Oceanic Technol.*, **29**, 89-102. [published, refereed]

Swales, D.J., G.S. Young, T.D. Sikora, N.S. Winstead, and H.N. Shirer, 2012: Synthetic aperture radar remote sensing of shear-driven atmospheric internal gravity waves in the vicinity of a warm front. *Mon. Wea. Rev.*, **140**, 1872-1882. [published, refereed]

Winstead, N.S., G.S. Young, and T.D. Sikora: Demonstration of the use of synthetic aperture radar-determined wind speed in numerical weather prediction error detection. *Natl. Wea. Dig.* [refereed]